SAND--82-1253C
Conf-820944--6

DISCLAIMER

This report was prepared as an account of work sponsored by an agency of the United States Government. Neither the United States Government nor any agency thereof, nor any of their employees, makes any warranty, express or implied, or assumes any legal liability or responsibility for the accuracy, completeness, or usefulness of any information, apparatus, product, or process disclosed, or represents that its use would not infringe privately owned rights. Reference herein to any specific commercial product, process, or service by trade name, trademark, manufacturer, or otherwise, does not necessarily constitute or imply its endorsement, recommendation, or favoring by the United States Government or any agency thereof. The views and opinions of authors expressed herein do not necessarily state or reflect those of the United States Government or any agency thereof.

SAND--82-1253C

DE82 021079

MASTER

DIAGNOSING ION-BEAM TARGETS, DATA ACQUISITION, REACTOR CONDITIONS*

C. W. Mendel, Jr.
Sandia National Laboratories, Albuquerque, NM 87185 (USA)

The final lecture will discuss diagnostics of the target. These are very difficult because of the short times, small spatial extent, and extreme values of temperture and pressure. Diagnostics for temperature, density profile, and neutron production will be discussed. A few minutes will be devoted to data acquisition needs. The lecture will end with a discussion of current areas where improvements are needed and future diagnostics that will be required for reactor conditions.

*This work was supported by the U. S. Department of Energy under contract DE-AC04-76-DP00789.

DISTRIBUTION OF THIS DOCUMENT IS UNLIMITED

DISCLAIMER

This report was prepared as an account of work sponsored by an agency of the United States Government. Neither the United States Government nor any agency Thereof, nor any of their employees, makes any warranty, express or implied, or assumes any legal liability or responsibility for the accuracy, completeness, or usefulness of any information, apparatus, product, or process disclosed, or represents that its use would not infringe privately owned rights. Reference herein to any specific commercial product, process, or service by trade name, trademark, manufacturer, or otherwise does not necessarily constitute or imply its endorsement, recommendation, or favoring by the United States Government or any agency thereof. The views and opinions of authors expressed herein do not necessarily state or reflect those of the United States Government or any agency thereof.

DISCLAIMER

Portions of this document may be illegible in electronic image products. Images are produced from the best available original document.

Figure 3.1 shows an ion beam target.[1] It consists of a layer of light metal slightly thicker than an ion range called the ablator which absorbs the energy of the ion beam. Inside of this layer is a layer called the pusher, which is made of heavy metal. It is driven inward by the pressure of the heated light metal layer. The pusher compresses the fusile gas (deuterium and tritium) inside of it. As the fusile gas is compressed, it is heated. When the gas becomes hot enough (10 keV) and dense enough so that an ion has a sufficiently high probability of being involved in a fusion reaction ($\rho r \sim 10^{23}$ cm^{-2}), the target will burn. The radii versus time of the various layers is shown schematically in Fig. 3.2. In this figure, T_p is the pulse length of the ion beam on the target and P is the power of that pulse. After target burn, the target expands and couples energy into the target chamber gas. The x-ray energy has by this time already been deposited in the gas. Figure 3.3 shows pressure profiles in the chamber gas at several times after the burn.[2] The pressure pulse is extremely high initially but by the time it reaches the wall it has expanded in volume so that the peak is roughly one atmosphere. The pressure pulse can be used to measure the energy of the burn.

No ion beam experiments on targets have been done with target chamber gas since we are using ion diodes which focus directly on the target. We have developed some of the needed diagnostics, however. The first parameter to measure is the uniformity of deposition of ion energy in the light metal outer shell. We presently use K-alpha emission of soft x-rays for this purpose.[3,4] Figure 3.4 shows this diagnostic. The ion beam is focused on a thin, sub-range foil of aluminum (8 μm thick for 1 MeV protons). The ions excite inner shell electrons of the aluminum. The excited aluminum ions then emit soft, 1.487 keV x-rays as they return to their ground states. These soft x-rays are recorded with a pinhole camera. Optical light, and ultra-violet light are filtered out with a 4 μm aluminum thin foil in front of the film. Hard x-rays are filtered out by using single emulsion films which are too thin for exposure by high energy x-rays.[5] Figure 3.5 shows data taken by this method. In this photograph there were actually two half-cones of different size showing the beam at two different radii. At the larger radius, the beam shows time-integrated spatial structure less than a millimeter in extent. At the smaller radius, beam mixing reduces the inhomogeneity and the structure is less apparent.

To use this technique in a reactor, K-alpha or M-alpha light from the front of the foil (the outer target shell) would be photographed. In a reactor situation the camera will need to be gated to avoid the much brighter x-rays from the burn. This will involve gating or exposure times of a few nanoseconds. We presently use x-ray cameras with 5 ns shutter times.[7] The development of this diagnostic for reactor conditions will be difficult since the camera will be outside the chamber, several meters from the target. The uniformity of deposition is a very important parameter since targets require energy deposition to be uniform to a few percent for the various targets considered. Development of this diagnostic is therefore quite important.

The symmetry of the implosion of the target can be monitored by flash x-radiography. The implosion symmetry is a product of the energy deposition symmetry, target symmetry, and implosion stability, so this diagnostic is more important than the K- or M-alpha diagnostic, but does not totally replace it. In this diagnostic a 3 ns burst[8] of $\sim$ 200 keV x-rays irradiate the the target at several different times during the implosion. The target is photographed with these x-rays by gated cameras.[6]

Figure 3.6 shows such a camera as employed on experiments on the Proto-I pulser at Sandia. The experiment employed three x-ray pulsers and three cameras. The cameras were gated with 5 ns gating pulses so they only show the data from the target x-ray pulse. Figure 3.7 shows a photograph of the target before implosion and three photographs during an implosion caused by an ion beam. Cylindrical targets also have been imploded with ion beams and photographed with the same system. They compare well to holographic data on similar targets. The technique gives 100 μm resolution, but must be improved to 10 μm for a reactor. Presently, the x-ray source and the cameras were much too close to the target (about 20 cm) for a reactor vessel. The diagnostic will have to be greatly improved for usefulness under reactor conditions. This will require more powerful, short-burst x-ray sources and more sensitive cameras. The cameras will need to be gated for somewhat shorter times since an implosion in a reactor should take 5 to 15 ns. This shorter gating time appears to be readily achievable.

The above measurements (ion deposition uniformity and implosion x-ray photographs) both require data to be recorded during periods of high electromagnetic, x-ray, and gamma-ray backgrounds. They will take place a hundred nanoseconds after the main power pulse on the diode, so it will not be during the bremsstrahlung pulse of the machine. However, the burn itself will also cause electromagnetic, x-ray, and gamma-ray backgounds. These diagnostics will require very careful shielding and the diagnostician must take every opportunity to make them insensitive to unwanted signals.

When the target burns it emits neutrons with the characteristic energy of the various reactions involved. There is a spread in the energy which is characteristic of the energy spread of the ions in the reaction. The measure of the energy spread is thus a measure of the burn temperature. The neutron energy and spread in energy are measured by the time-of-flight, and the spread in the time-of-flight to neutron detectors.[9] The time-of-flight will be hundreds of nanoseconds as opposed to the few nanoseconds for x-rays. It is therefore easy to discriminate between them. The x-rays in fact provide a convenient fiducial for the measurement.

Measurement of x-ray and debris energy from the target chamber shock wave[2] should be straightforward. Many detectors are available with high electric output, and all of the various noise pulses should be well over by the time the pressure pulse reaches the chamber wall. Piezoelectric pressure gauges, for example, are very rugged and reliable.

I would like to say a few words about data acquisition. The largest ion beam fusion accelerator presently in operation is the PBFA-I accelerator mentioned in the first lecture. Data from diagnostics with fast electrical output are presently recorded on 40 Tektronix 7912 digitizing oscilloscopes. In addition there are 350 channels of single point data (amplitude at a given time or time at which a specified amplitude was reached) recorded by a Camac system.[10] The system will soon be expanded to sixty digital oscilloscopes and will still be considered marginal by some of us. Good, high volume data recording and analyzing systems are indispensible. The cabling must be high quality, double-shielded, low dispersion coaxial cable protected from excessive x-ray dosage. Routines will be needed to compensate for cable dispersion. All splices must be made in carefully contructed junction boxes, and the computer and recording equipment must be in a high quality shielded room. Personnel must be protected from x-ray and eventually neutron pulses at the same time. In the future, fiber optic data transmission should improve noise levels on the data. Finally, every effort must be made to get as much as possible from the data by extensive theoretical modeling. Although a large number of data channels can compensate somewhat for the lack of a good model, these data acquisition systems are very expensive and more importantly, require extensive maintenance.

Many of the diagnostics give a pictorial output such as an x-ray photograph. Digitizing diode arrays mentioned in the second lecture will allow this data to be fed directly to the computer. However, these devices work by storing charge, so x-ray shielding will be essential.

All of the diagnostics mentioned in these lectures need further development. Some of them, like the diagnosis of the power flow in the transmission lines where electron flow is important, require improved modeling. In situ diagnosis of the electron cloud in ion diodes is important right now and no diagnostic is available. Hopefully the diodes will be so well understood and reliable by the time they are in reactors that there will be no need for such diagnostics. The diagnosis of ion transport channels with holography is in relatively good shape. It should be possible to diagnose all of the channels with holograms along perhaps three axes. Diagnosis of the channels with spectroscopy has not yet begun and is a fertile field for development. The resolution and stand-off distance of target diagnostics must be improved for both near term and reactor applications. Some of these (e.g., K- or M-alpha photographs) involve x-ray pinhole cameras which will need to be replaced by small angle elliptical mirrored cameras like those used in high-altitude x-ray telescopes and laser fusion x-ray dignostics.[11]

Light ion beam fusion has a problem with the high bremsstrahlung radiation of the pulsed power. However, it also has a great advantage in that the pulsed power is separated from the pulse on target by several hundred nanoseconds and the target x-rays and gamma rays are separated from the neutron pulse by several hundred nanoseconds. The hardening of diagnostics is thus simplified. Data storing devices such as diode digitizer arrays will still need careful shielding however.

References

1. M. J. Clauser, Phys. Rev. Lett. 35, 848 (1975).
2. S. I. Abdel-Khalik, G. A. Moses, and R. R. Peterson, Nuclear Engineeing and Design 63, 315 (1981).
3. D. J. Johnson, G. W. Kuswa, A. V. Farnsworth, Jr., J. P. Quintenz, R. J. Leeper, E. J. T. Burns, and S. Humphries, Jr., Phys. Rev. Lett. 42, 610 (1979).
4. R. D. Bleach, D. J. Nagal, D. Mosher, and S. J. Stephanakis, J. Appl. Phys. 52, 3064 (1981).
5. E. J. T. Burns, private communication.
6. D. L. Fehl, J. Chang, G. W. Kuswa, and C. W. Mendel, Jr., Rev. Sci. Inst. 51, 2921 (1980).
7. M. M. Widner, private communication.
8. J. Chang, D. L. Fehl, M. M. Widner, K. W. Bieg, and M. A. Palmer, Appl. Phys. Lett. 39, 224 (1981).
9. F. C. Young, D. J. Mosher, S. J. Stephanakis, S. A. Goldstein, and D. Hinshelwood, U. S. Naval Research Report 3823, August 1978.
10. E. L. Neau and W. B. Boyer, Proc. of the 3rd IEEE Int'l Pulsed Power Conf., 1981.
11. M. J. Boyle, Laser Fusion X-Ray Microscopy in Laser Fusion Annual Report-1976, Lawrence Livermore Laboratory, Rept. UCRL-50021-76 (1977) and M. Boyle and H. Ahlstrom, Rev. Sci. Inst. 49, 746 (1978).

Figure Captions

3-1. Schematic of an ion beam target implosion. The ion beam heats the ablator which is slightly longer than an ion range. The heated ablator drives the pusher inward which compresses the deuterium-tritium fuel mass. The target is about 1 cm in diameter.

3-2. The radii of the inner and outer boundaries of the ablator, pusher, and fuel mass versus time. T is the ion beam pulse length on target, P is the ion beam power on target. Figures 3.1 and 3.2 courtesy of M. M. Widner and A. V. Farnsworth, Jr.

3-3. Target chamber pressure for several different times after target burn. The initial pressure before burn was 100 Torr and the burn energy in debris was 30 MJ.

3-4. Experiment using K-alpha atomic excitation of a thin aluminum foil to look at beam uniformity. The beam excites the conical foil which is then photographed in the 1.487 keV k-alpha line with the pinhole camera.

3-5. K-alpha line photograph of two conical targets of different diameter showing the beam profile at 1.0 cm and 0.6 cm. Notice the detail in the larger diameter foil.

3-6. Schematic of a flash x-radiography experiment. The photo-electrons of the input cathode are multiplied by the input microchannel plate. The output of that plate is accelerated and then guided to the output plate by a magnetic field where it is multiplied again, accelerated to a phosphor and photographed.

3-7. Radiographs of the initial target, and at three later times using the apparatus in Fig. 3.6. The resolution can be judged by the expanding tungsten stalk visible in the last photograph.

PELLET IMPLOSION

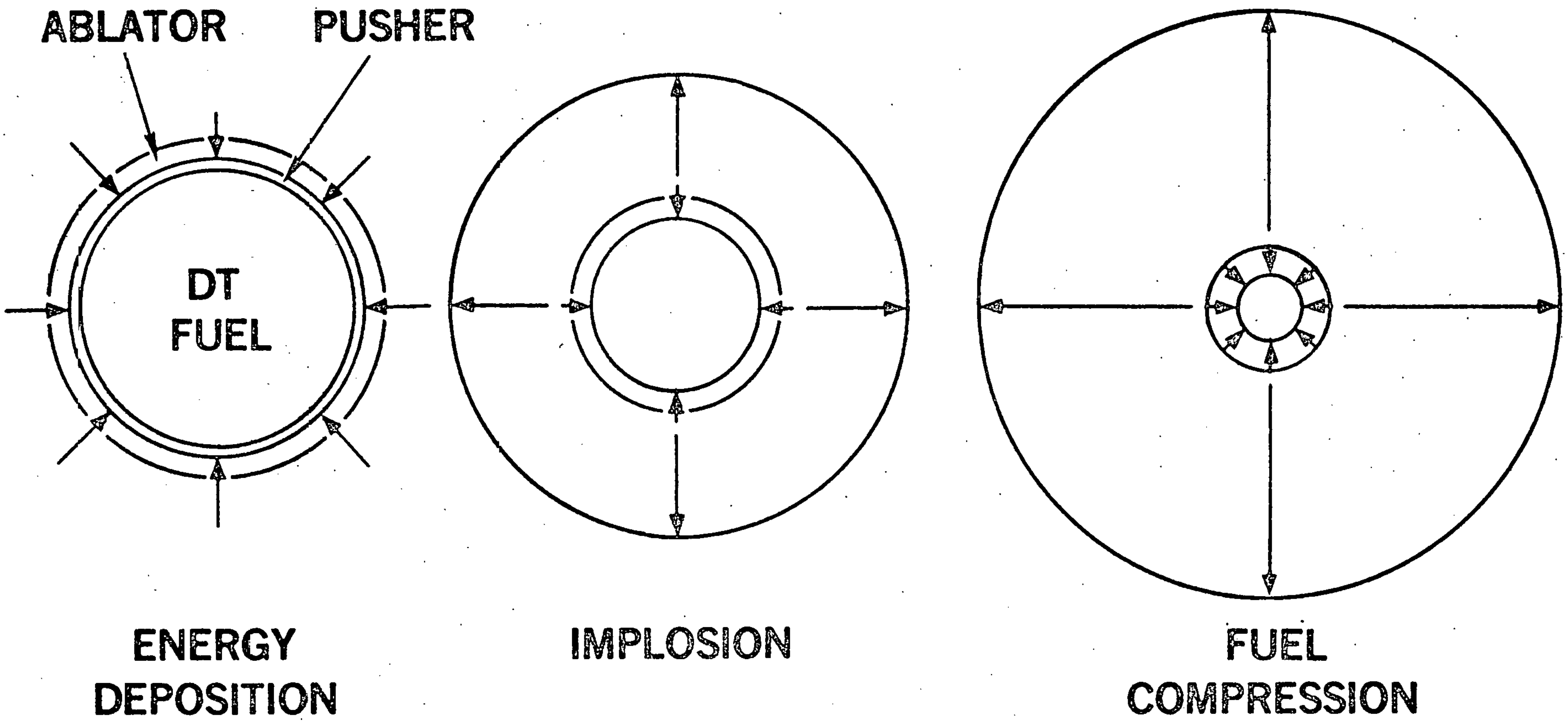

Sandia National Laboratories

MMW 3/82

IDEAL IMPLOSION

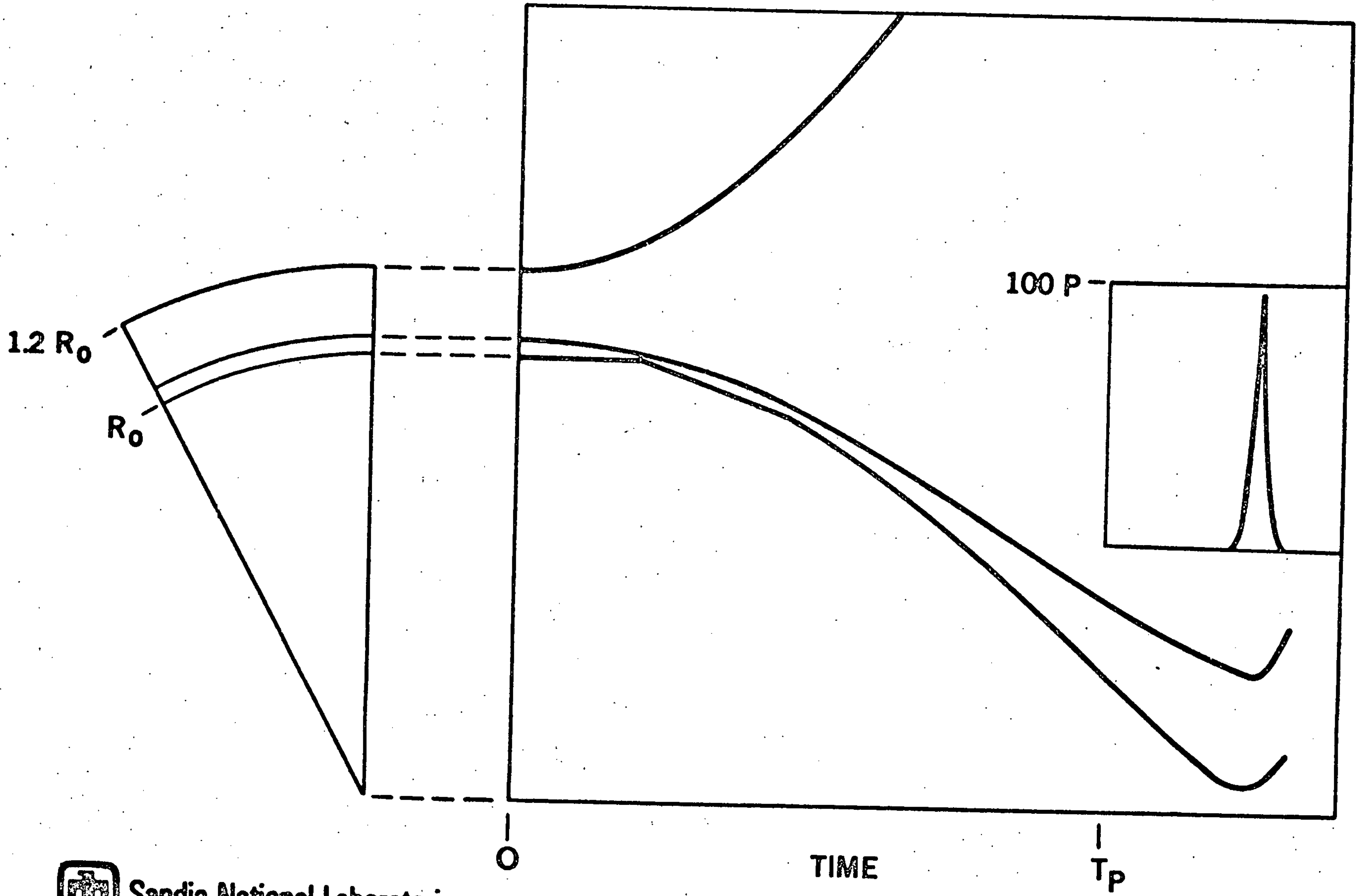

Sandia National Laboratories

AVF 3/82

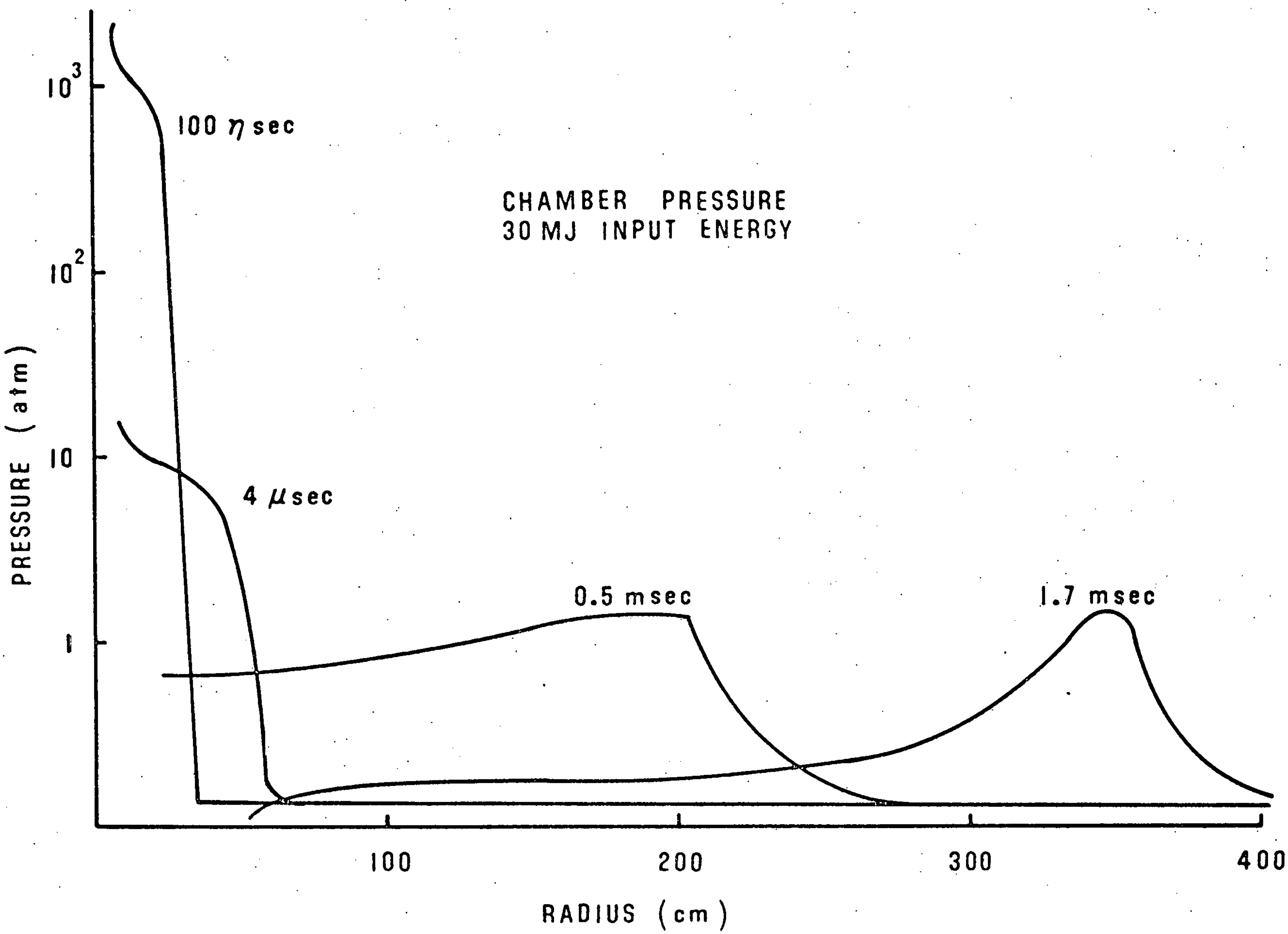

CHAMBER PRESSURE
30 MJ INPUT ENERGY
PRESSURE (atm)
10^3
10^2
10
1
100 η sec
4 μsec
0.5 msec
1.7 msec
100
200
300
400
RADIUS (cm)

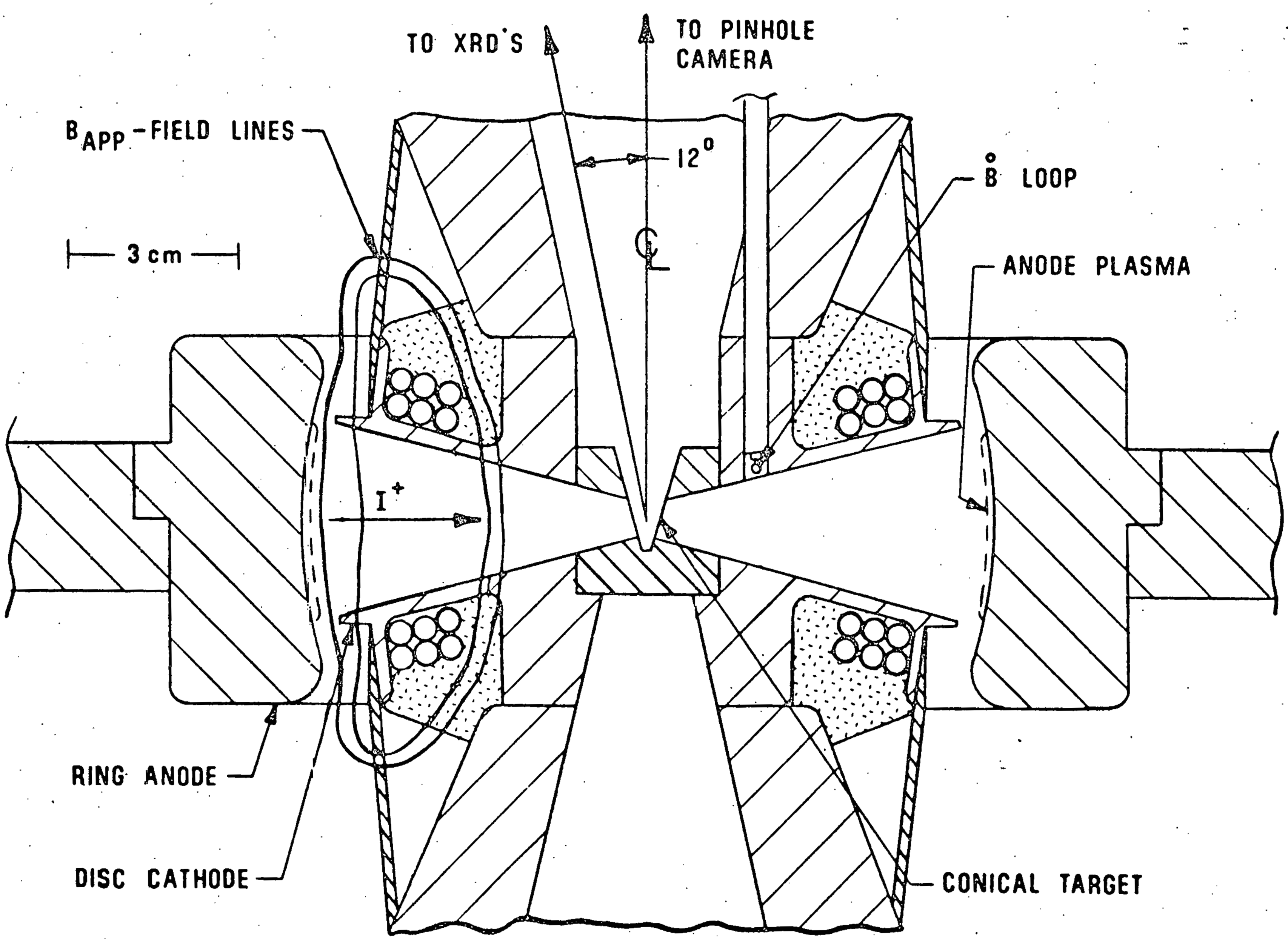
TO XRD'S
TO PINHOLE CAMERA
B_{APP}-FIELD LINES
12°
$\dot{B}$ LOOP
3 cm
ANODE PLASMA
I^+
RING ANODE
DISC CATHODE
CONICAL TARGET

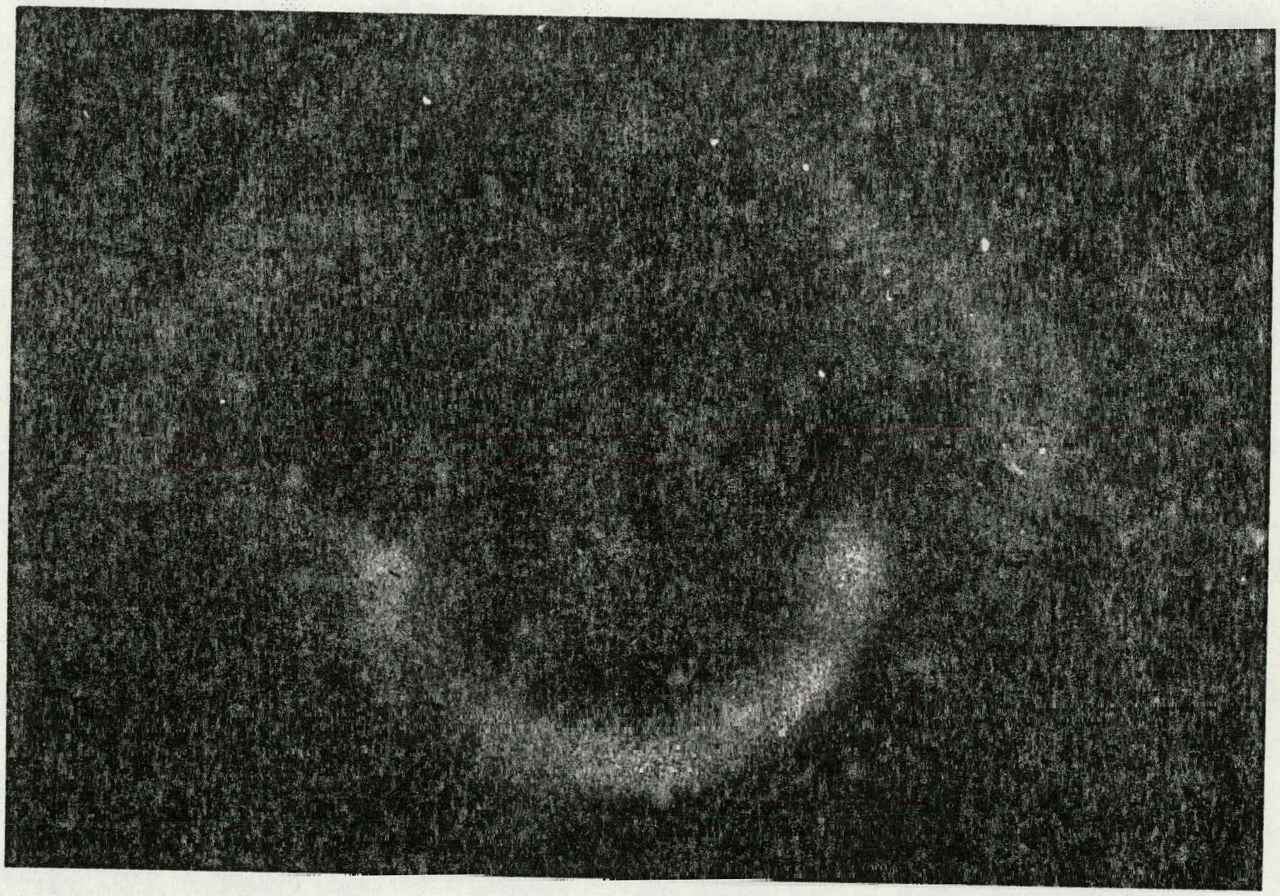

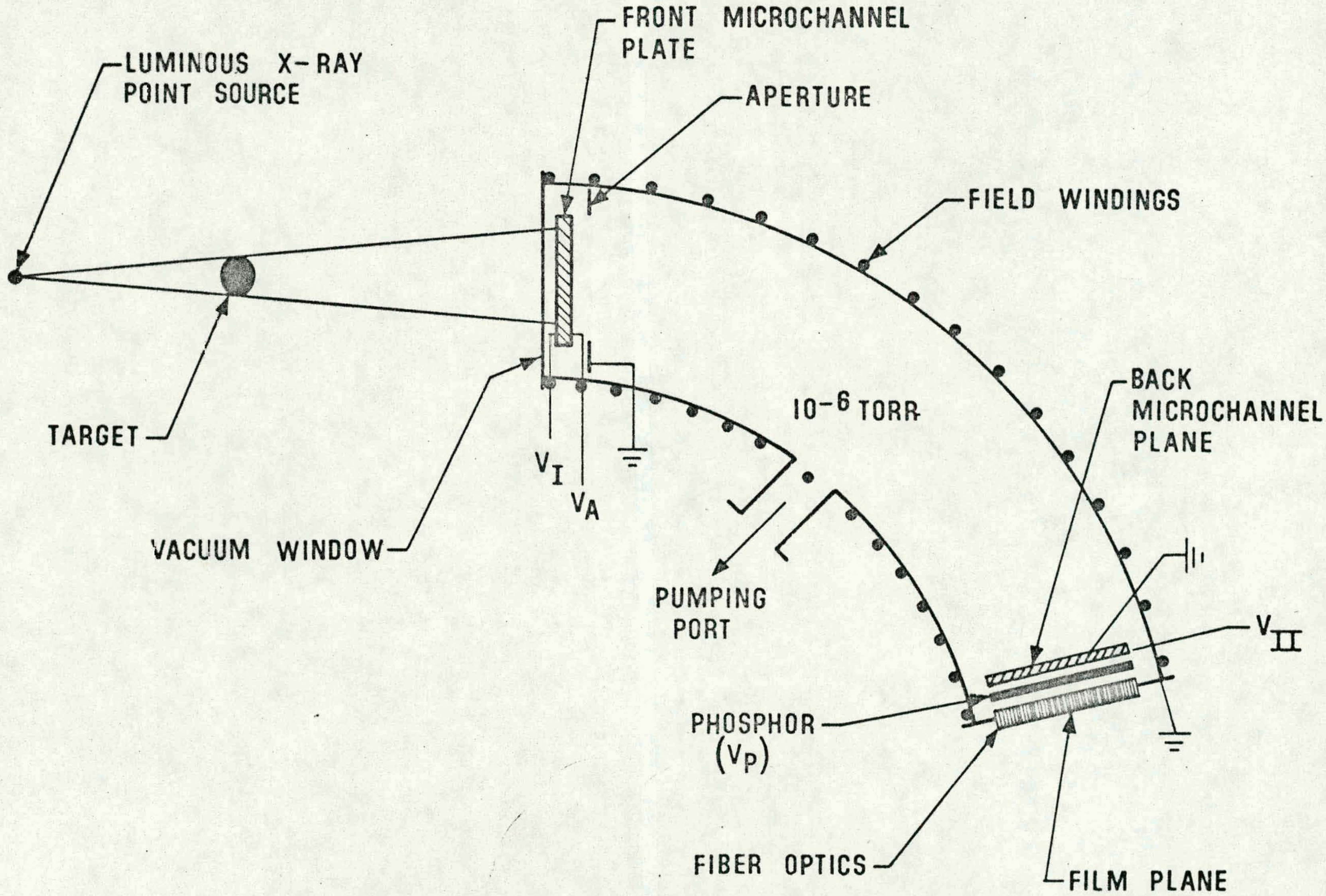

FRONT MICROCHANNEL PLATE
LUMINOUS X-RAY POINT SOURCE
APERTURE
FIELD WINDINGS
BACK MICROCHANNEL PLANE
10^-6 TORR
TARGET
V_I
V_A
VACUUM WINDOW
PUMPING PORT
V_{II}
PHOSPHOR (V_P)
FIBER OPTICS
FILM PLANE

SHOT 3268 PROTO I
Au SPHERE 25μm WALL